EPJ Web of Conferences **192**, 00035 (2018) https://doi.org/10.1051/epjconf/201819200035
QCD@Work 2018

Study of $\Upsilon(1S)$ radiative decays to $\gamma\pi^+\pi^-$ and γK^+K^-

Antimo Palano[1,*]

[1] *INFN and University of Bari, Via Orabona 4, 70125 Bari, Italy*

Abstract. We study the $\Upsilon(1S)$ radiative decays to $\gamma\pi^+\pi^-$ and γK^+K^- using data recorded with the *BABAR* detector operating at the SLAC PEP-II asymmetric-energy e^+e^- collider at center-of-mass energies at the $\Upsilon(2S)$ and $\Upsilon(3S)$ resonances. The $\Upsilon(1S)$ resonance is reconstructed from the decay $\Upsilon(nS) \to \pi^+\pi^-\Upsilon(1S)$, $n = 2, 3$.

1 Introduction

The existence of gluonium states is still an open issue for Quantum Chromodynamics (QCD). Lattice QCD calculations predict the lightest gluonium states to have quantum numbers $J^{PC} = 0^{++}$ and 2^{++} and to be in the mass region below 2.5 GeV/c^2 [1]. In particular, the $J^{PC} = 0^{++}$ glueball is predicted to have a mass around 1.7 GeV/c^2. Radiative decays of heavy quarkonia, in which a photon replaces one of the three gluons from the strong decay of J/ψ or $\Upsilon(1S)$, can probe color-singlet two-gluon systems that produce gluonic resonances. J/ψ decays have been extensively studied in the past [2]. In this analysis [3] we study $\Upsilon(1S)$ decays, taking into account that the experimental observation of radiative $\Upsilon(1S)$ decays is challenging because their rate is suppressed by a factor of ≈ 0.025 compared to J/ψ radiative decays, which are of order 10^{-3} [4].

2 Events reconstruction

We reconstruct the decay chains

$$\Upsilon(2S)/\Upsilon(3S) \to (\pi_s^+\pi_s^-)\Upsilon(1S) \to (\pi_s^+\pi_s^-)(\gamma\pi^+\pi^-) \tag{1}$$

and

$$\Upsilon(2S)/\Upsilon(3S) \to (\pi_s^+\pi_s^-)\Upsilon(1S) \to (\pi_s^+\pi_s^-)(\gamma K^+K^-), \tag{2}$$

where we label with the subscript s the slow pions from the direct $\Upsilon(2S)$ and $\Upsilon(3S)$ decays.

Events with balanced momentum are required to satisfy energy balance requirements. For each combination of $\pi_s^+\pi_s^-$ candidates, we first require both particles to be identified loosely as pions and compute the recoiling mass

$$M^2_{\rm rec}(\pi_s^+\pi_s^-) = |p_{e^+} + p_{e^-} - p_{\pi_s^+} - p_{\pi_s^-}|^2, \tag{3}$$

where p is the particle four-momentum. The distribution of $M^2_{\rm rec}(\pi_s^+\pi_s^-)$ is expected to peak at the squared $\Upsilon(1S)$ mass for signal events. Figure 1 shows the combinatorial recoiling mass $M_{\rm rec}(\pi_s^+\pi_s^-)$ for $\Upsilon(2S)$ and $\Upsilon(3S)$ data, where narrow peaks at the $\Upsilon(1S)$ mass can be observed.

* e-mail: antimo.palano@ba.infn.it

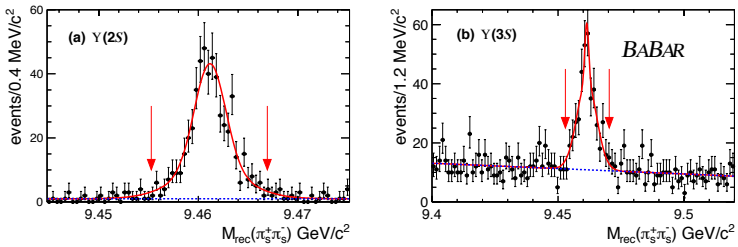

Figure 1. Combinatorial recoiling mass $M_{\rm rec}$ to $\pi_s^+\pi_s^-$ candidates for (a) $\Upsilon(2S)$ and (b) $\Upsilon(3S)$ data.

We select signal event candidates by requiring

$$|M_{\rm rec}(\pi_s^+\pi_s^-) - m(\Upsilon(1S))_f| < 2.5\sigma, \tag{4}$$

where $m(\Upsilon(1S))_f$ indicates the fitted $\Upsilon(1S)$ mass value. To reconstruct $\Upsilon(1S) \to \gamma\pi^+\pi^-$ or $\Upsilon(1S) \to \gamma K^+K^-$ decays, we require a loose identification of both pions or kaons and isolate the decays by requiring

$$9.1\ \text{GeV}/c^2 < m(\gamma h^+h^-) < 9.6\ \text{GeV}/c^2, \tag{5}$$

where $h = \pi, K$.

3 Study of the $\pi^+\pi^-$ and K^+K^- mass spectra

The $\pi^+\pi^-$ mass spectrum, for $m(\pi^+\pi^-) < 3.0$ GeV/c^2 and summed over the $\Upsilon(2S)$ and $\Upsilon(3S)$ datasets with 507 and 277 events, respectively, is shown in Fig. 2(Left). The spectrum shows $I = 0$, $J^P = \text{even}^{++}$ resonance production, with low backgrounds above 1 GeV/c^2. We observe a rapid drop around 1 GeV/c^2 characteristic of the presence of the $f_0(980)$, and a strong $f_2(1270)$ signal. The data also suggest the presence of weaker resonant contributions.

The K^+K^- mass spectrum, summed over the $\Upsilon(2S)$ and $\Upsilon(3S)$ datasets with 164 and 63 events, respectively, is shown in Fig. 2(Right) and also shows resonant production, with low background. Signals at the positions of $f_2'(1525)$ and $f_0(1710)$ can be observed.

We make use of a phenomenological model to extract the different $\Upsilon(1S) \to \gamma R$ branching fractions, where R is an intermediate resonance. We perform a simultaneous binned fit to the $\pi^+\pi^-$ mass spectra from the $\Upsilon(2S)$ and $\Upsilon(3S)$ datasets. We describe the low-mass region (around the $f_0(500)$) using a relativistic S-wave Breit-Wigner lineshape having free parameters. We describe the $f_0(980)$ using the Flatté [6] formalism. The $f_2(1270)$ and $f_0(1710)$ resonances are represented by relativistic Breit-Wigner functions with parameters fixed to PDG values [7]. In the high $\pi^+\pi^-$ mass region we include a single resonance $f_0(2100)$ having a width fixed to the PDG value (224 ± 22) and unconstrained mass. For the $\Upsilon(3S)$ data we also include $\rho(770)^0$ background with parameters fixed to the PDG values. The fit is shown in Fig. 2. It has 16 free parameters and $\chi^2 = 182$ for ndf=152, corresponding to a p-value of 5%. We note the observation of a significant S-wave in $\Upsilon(1S)$ radiative decays. This observation was not possible in the study of J/ψ radiative decay to $\pi^+\pi^-$ because of the presence of a strong, irreducible background from $J/\psi \to \pi^+\pi^-\pi^0$ [8]. No evidence is found for a $\Upsilon(1S) \to \pi^+\pi^-\pi^0$ decay in present data. We obtain the following $f_0(500)$ parameters:

$$m(f_0(500)) = 0.856 \pm 0.086\ \text{GeV}/c^2, \Gamma(f_0(500)) = 1.279 \pm 0.324\ \text{GeV}, \tag{6}$$

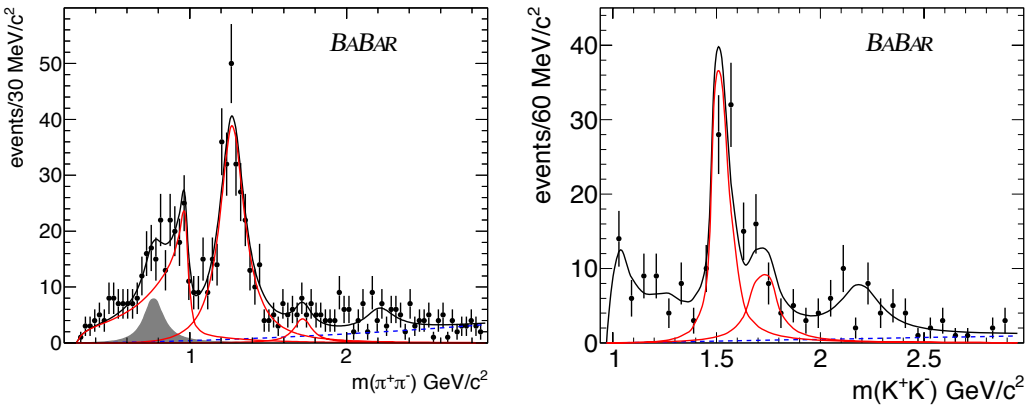

Figure 2. (Left) $\pi^+\pi^-$ mass distribution from $\Upsilon(1S) \to \pi^+\pi^-\gamma$ for the combined $\Upsilon(2S)$ and $\Upsilon(3S)$ datasets. The full (red) curves indicate the S-wave, $f_2(1270)$, and $f_0(1710)$ contributions. The shaded (gray) area represents the fitted $\rho(770)^0$ background. (Right) K^+K^- mass distribution from $\Upsilon(1S) \to K^+K^-\gamma$ for the combined $\Upsilon(2S)$ and $\Upsilon(3S)$ datasets. The (red) curves show the contributions from $f_2'(1525)$ and $f_0(1710)$. Dashed (blue) lines indicate the background contributions.

and $\phi = 2.41 \pm 0.43$ rad. The fraction of S-wave events associated with the $f_0(500)$ is $(27.7 \pm 3.1)\%$.

We perform a binned fit to the combined K^+K^- mass spectrum using the following model. The $f_0(980)$ is parameterized according to the Flatté formalism. The $f_2(1270)$, $f_2'(1525)$, $f_0(1500)$, and $f_0(1710)$ resonances are represented by relativistic Breit-Wigner functions with parameters fixed to PDG values. We include an $f_0(2200)$ contribution having parameters fixed to the PDG values. The fit shown in Fig. 2(Right). It has six free parameters and $\chi^2 = 35$ for ndf=29, corresponding to a p-value of 20%. The resonances yields and significances are given in Table 1. Systematic uncertainties are dominated by the PDG uncertainties on resonances parameters.

Table 1. Resonances yields and statistical significances from the fits to the $\pi^+\pi^-$ and K^+K^- mass spectra for the $\Upsilon(2S)$ and $\Upsilon(3S)$ datasets. The symbol $f_J(1500)$ indicates the signal in the 1500 MeV/c^2 mass region.

Resonances ($\pi^+\pi^-$)	Yield $\Upsilon(2S)$	Yield $\Upsilon(3S)$	Significance
S-wave	$133 \pm 16 \pm 13$	87 ± 13	12.8σ
$f_2(1270)$	$255 \pm 19 \pm 8$	$77 \pm 7 \pm 4$	15.9σ
$f_0(1710)$	$24 \pm 8 \pm 6$	$6 \pm 8 \pm 3$	2.5σ
Resonances (K^+K^-)	Yield $\Upsilon(2S) + \Upsilon(3S)$		Significance
$f_0(980)$	47 ± 9		5.6σ
$f_J(1500)$	$77 \pm 10 \pm 10$		8.9σ
$f_0(1710)$	$36 \pm 9 \pm 6$		4.7σ

4 Efficiency correction

The efficiency distributions as functions of mass, for the $\Upsilon(2S)/\Upsilon(3S)$ data and for the $\pi^+\pi^-\gamma$ and $K^+K^-\gamma$ final states, are found to have an almost uniform behavior for all the final states. We define the helicity angle θ_H as the angle formed by the h^+, in the h^+h^- rest frame, and the γ in the $h^+h^-\gamma$ rest frame. We also define θ_γ as the angle formed by the radiative photon in the $h^+h^-\gamma$ rest frame with respect to the $\Upsilon(1S)$ direction in the $\Upsilon(2S)/\Upsilon(3S)$ rest frame. We label with $\epsilon(m, \cos\theta_H)$ the efficiency computed as a function of the h^+h^- effective mass and the helicity angle $\cos\theta_H$. This is used only to obtain efficiency-corrected mass spectra. We label with $\epsilon(\cos\theta_H, \cos\theta_\gamma)$ the efficiency computed, for each resonance mass window, as a function of $\cos\theta_H$ and $\cos\theta_\gamma$. This is used to obtain the efficiency-corrected angular distributions and branching fractions of the different resonances. To obtain the efficiency correction weight w_R for the resonance R we divide each event by the efficiency $\epsilon(\cos\theta_H, \cos\theta_\gamma)$

$$w_R = \frac{\sum_{i=1}^{N_R} 1/\epsilon_i(\cos\theta_H, \cos\theta_\gamma)}{N_R}, \tag{7}$$

where N_R is the number of events in the resonance mass range.

5 Angular analysis

To obtain information on the angular momentum structure of the $\pi^+\pi^-$ and K^+K^- systems in $\Upsilon(1S) \to \gamma h^+h^-$ we study the dependence of the $m(h^+h^-)$ mass on the helicity angle θ_H. A better way to observe angular effects is to plot the $\pi^+\pi^-$ mass spectrum weighted by the Legendre polynomial moments, corrected for efficiency and shown in Fig. 3. In a simplified environment, the moments are related to the spin 0 (S) and spin 2 (D) amplitudes by the equations [9]:

$$\begin{aligned}
\sqrt{4\pi}\langle Y_0^0\rangle &= S^2 + D^2, \\
\sqrt{4\pi}\langle Y_2^0\rangle &= 2SD\cos\phi_{SD} + 0.639D^2, \\
\sqrt{4\pi}\langle Y_4^0\rangle &= 0.857D^2,
\end{aligned} \tag{8}$$

where ϕ_{SD} is the relative phase. Therefore we expect to observe spin 2 resonances in $\langle Y_4^0\rangle$ and S/D interference in $\langle Y_2^0\rangle$. The results are shown in Fig. 3(Top). We clearly observe the $f_2(1270)$ resonance in $\langle Y_4^0\rangle$ and a sharp drop in $\langle Y_2^0\rangle$ at the $f_2(1270)$ mass, indicating the interference effect. The distribution of $\langle Y_0^0\rangle$ is just the scaled $\pi^+\pi^-$ mass distribution, corrected for efficiency. Similarly, we plot in Fig. 3(Bottom) the K^+K^- mass spectrum weighted by the Legendre polynomial moments, corrected for efficiency. We observe signals of the $f_2'(1525)$ and $f_0(1710)$ in $\langle Y_4^0\rangle$ and activity due to S/D interference effects in the $\langle Y_2^0\rangle$ moment.

Resonance angular distributions in radiative $\Upsilon(1S)$ decays from $\Upsilon(2S)/\Upsilon(3S)$ decays are rather complex. In this section we perform a simplified Partial Wave Analysis (PWA) solving directly the system of Eq. (8). Figure 4 shows the resulting S-wave and D-wave contributions to the $\pi^+\pi^-$ and K^+K^- mass spectra, respectively. Due to the presence of background in the threshold region, the $\pi^+\pi^-$ analysis is performed only on the $\Upsilon(2S)$ data.

We note that in the case of the $\pi^+\pi^-$ mass spectrum we obtain a good separation between S and D-waves, with the presence of an $f_0(980)$ resonance on top of a broad $f_0(500)$ resonance in the S-wave and a clean $f_2(1270)$ in the D-wave distribution. Integrating the S-wave amplitude from threshold up to a mass of 1.5 GeV/c^2, we obtain an integrated, efficiency corrected yield $N(S\text{-wave}) = 629 \pm 128$.

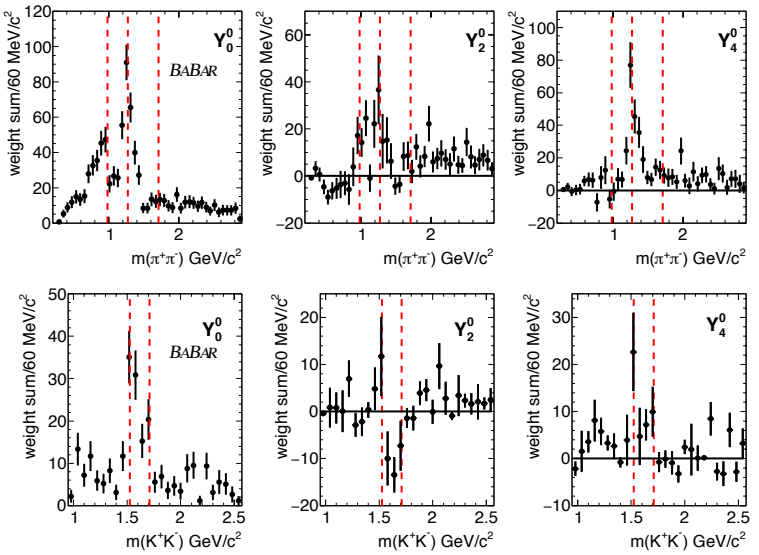

Figure 3. The distributions of the most relevant unnormalized Y_L^0 moments for $\Upsilon(1S) \to \gamma\pi^+\pi^-$ (Top) and $\Upsilon(1S) \to \gamma K^+K^-$ (Bottom) as functions of mass. The lines indicate the positions of $f_0(980)$, $f_2(1270)$, and $f_0(1710)$ for $\pi^+\pi^-$ and $f_2'(1525)$ and $f_0(1710)$ for K^+K^-.

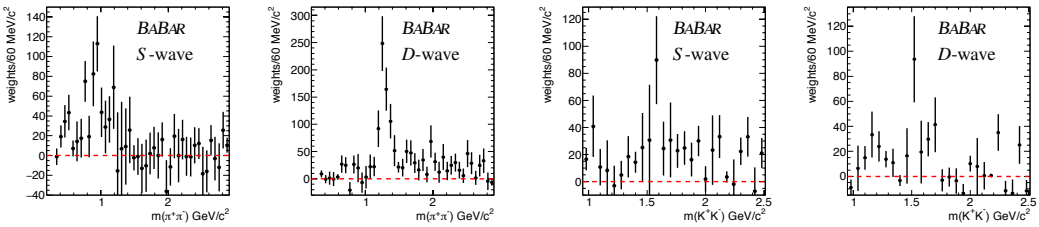

Figure 4. S and D-wave contributions from the simple PWA of the $\pi^+\pi^-$ mass spectrum for the $\Upsilon(2S)$ data (Left) and of the K^+K^- mass spectrum for the combined $\Upsilon(2S)/\Upsilon(3S)$ data (Right).

In the case of the K^+K^- PWA the structure peaking around 1500 MeV/c^2 appears in both S and D-waves suggesting the presence of $f_0(1500)$ and $f_2'(1525)$. In the $f_0(1710)$ mass region there is not enough data to discriminate between the two different spin assignments. This pattern is similar to that observed in the Dalitz plot analysis of charmless $B \to 3K$ decays [10]. Integrating the S and D-wave contributions in the $f_2'(1525)/f_0(1500)$ mass region, we obtain a fraction of S-wave contribution $f_S(K^+K^-) = 0.53 \pm 0.10$.

The full $\Upsilon(nS)$ angular distributions for decays Eq. (1) and Eq. (2) are expressed in terms of θ_γ and θ_H where the $\Upsilon(1S)$ can be produced with helicity 0 or 1. A spin 2 resonance, on the other hand, can have three helicity states. We make use of the helicity formalism [11, 12] to derive the angular distributions for a spin 2 and spin 0 resonance as reported in Ref. [3]. We perform a 2D unbinned maximum likelihood fit for each resonance using the spin 2 and spin 0 full angular distributions. We

first fit the $f_2(1270)$ angular distributions and allow a background contribution of 16% from the S-wave having fixed parameters. Figure 5 shows the uncorrected fit projections on $\cos\theta_H$ and $\cos\theta_\gamma$. The $\cos\theta_\gamma$ spectrum is approximately uniform, while $\cos\theta_H$ shows structures well-fitted by the spin 2 hypothesis.

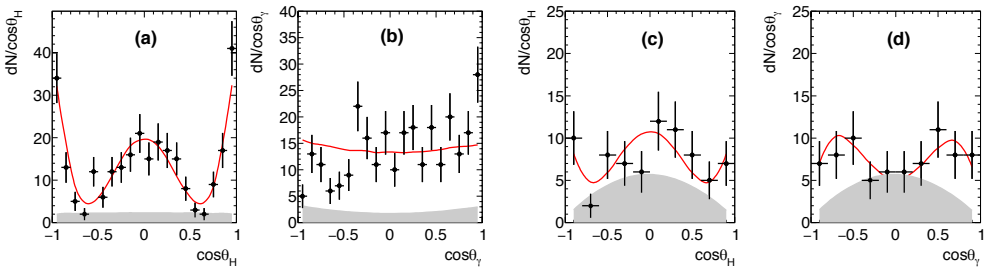

Figure 5. Uncorrected (a) $\cos\theta_H$ and (b) $\cos\theta_\gamma$ distributions in the $f_2(1270) \to \pi^+\pi^-$ mass region. Uncorrected (c) $\cos\theta_H$ and (d) $\cos\theta_\gamma$ distributions in the $f_J(1500) \to K^+K^-$ mass region. The full (red) lines are the projections from the fit with the spin 2 hypothesis. The shaded (gray) area represents the S-wave contribution.

We fit the K^+K^- data in the $f_J(1500)$ mass region, where many resonances can contribute: $f_2'(1525)$, $f_0(1500)$ [10], and $f_0(1710)$. We fit the data using a superposition of S and D waves, having helicity contributions as free parameters, and free S-wave contribution. We obtain an S-wave contribution of $f_S(K^+K^-) = 0.52 \pm 0.14$, in agreement with the estimate obtained from the simple PWA. Fit projections are shown in Fig. 5, giving an adequate description of the data.

6 Measurement of branching fractions

We determine the branching fraction $\mathcal{B}(R)$ for the decay of $\Upsilon(1S)$ to photon and resonance R using the expression

$$\mathcal{B}(R) = \frac{N_R(\Upsilon(nS) \to \pi_s^+\pi_s^-\Upsilon(1S)(\to R\gamma))}{N(\Upsilon(nS) \to \pi_s^+\pi_s^-\Upsilon(1S)(\to \mu^+\mu^-))} \times \mathcal{B}(\Upsilon(1S) \to \mu^+\mu^-), \tag{9}$$

where N_R indicates the efficiency-corrected yield for the given resonance. To reduce systematic uncertainties, we first compute the relative branching fraction to the reference channel $\Upsilon(nS) \to \pi^+\pi^-\Upsilon(1S)(\to \mu^+\mu^-)$, which has the same number of charged particles as the final states under study. We then multiply the relative branching fraction by the well-measured branching fraction $\mathcal{B}(\Upsilon(1S) \to \mu^+\mu^-) = 2.48 \pm 0.05\%$ [7].

We determine the reference channel corrected yield using the method of "B-counting", also used to obtain the number of produced $\Upsilon(2S)$ and $\Upsilon(3S)$ [5]. Taking into account the known branching fractions of $\Upsilon(2S)/\Upsilon(3S) \to \pi_s^+\pi_s^-\Upsilon(1S)$ we obtain

$$N(\Upsilon(2S) \to \pi_s^+\pi_s^-\Upsilon(1S)(\to \mu^+\mu^-)) = (4.35 \pm 0.12_{\rm sys}) \times 10^5 \tag{10}$$

and

$$N(\Upsilon(3S) \to \pi_s^+\pi_s^-\Upsilon(1S)(\to \mu^+\mu^-)) = (1.32 \pm 0.04_{\rm sys}) \times 10^5 \tag{11}$$

events. Table 2 gives the measured branching fractions. In all cases we correct the efficiency corrected yields for isospin and for PDG measured branching fractions [7]. We report the first observation of

Table 2. Measured $\Upsilon(1S) \to \gamma R$ branching fractions.

Resonance	$\mathcal{B}(10^{-5})$
$\pi\pi$ S-wave	$4.63 \pm 0.56 \pm 0.48$
$f_2(1270)$	$10.15 \pm 0.59\ ^{+0.54}_{-0.43}$
$f_0(1710) \to \pi\pi$	$0.79 \pm 0.26 \pm 0.17$
$f_J(1500) \to K\bar{K}$	$3.97 \pm 0.52 \pm 0.55$
$f_2'(1525)$	$2.13 \pm 0.28 \pm 0.72$
$f_0(1500) \to K\bar{K}$	$2.08 \pm 0.27 \pm 0.65$
$f_0(1710) \to K\bar{K}$	$2.02 \pm 0.51 \pm 0.35$

$f_0(1710)$ in $\Upsilon(1S)$ radiative decay with a significance of 5.7σ, combining $\pi^+\pi^-$ and K^+K^- data. To determine the branching ratio of the $f_0(1710)$ decays to $\pi\pi$ and $K\bar{K}$, we remove all the systematic uncertainties related to the reference channels and of the γ reconstruction. Labelling with N the efficiency-corrected yields for the two $f_0(1710)$ decay modes, we obtain

$$\frac{\mathcal{B}(f_0(1710) \to \pi\pi)}{\mathcal{B}(f_0(1710) \to K\bar{K})} = \frac{N(f_0(1710) \to \pi\pi)}{N(f_0(1710) \to K\bar{K})} = 0.64 \pm 0.27_{\text{stat}} \pm 0.18_{\text{sys}}, \tag{12}$$

in agreement with the world average value of $0.41^{+0.11}_{-0.17}$ [7].

These results may contribute to the long-standing issue of the identification of a scalar glueball.

References

[1] Y. Chen *et al.* Phys. Rev. D **73**, 014516 (2006).
[2] L. Köpke and N. Wermes, Phys. Rept. **174**, 67 (1989).
[3] J. P. Lees *et al.* [BaBar Collaboration], Phys. Rev. D **97** (2018) no.11, 112006
[4] S.B. Athar *et al.* (CLEO Collaboration), Phys. Rev. D **73**, 032001 (2006).
[5] Ed. A.J. Bevan, B. Golob, Th. Mannel, S. Prell, and B.D. Yabsley, "*The Physics of the B Factories*", Eur. Phys. J. C **74**, 302 (2014).
[6] S.M. Flatté, Phys. Lett. B **63**, 224 (1976).
[7] C. Patrignani *et al.* (Particle Data Group), Chin. Phys. C **40**, 100001 (2016).
[8] J. Becker *et al.* (Mark III Collaboration), Phys. Rev. D **35**, 2077 (1987).
[9] G. Costa *et al.* Nucl. Phys. B**175** 402 (1980).
[10] J.P. Lees *et al.* (*BABAR* Collaboration), Phys.Rev. D **85**, 112010 (2012).
[11] L. Breva-Newell, "Decays of the $\Upsilon(1S)$ into a photon and two charged hadrons", PhD thesis, hep-ex/0412075 (2004).
[12] J.D. Richman, "An Experimenter's Guide to the Helicity Formalism", CALT-68-1148 (1984).
[13] W. M. Yao *et al.* (Particle Data Group), J. Phys. G **33**, 1 (2006).